Analysis on surface characteristics of electro-discharge machined Inconel 718

Rahul

Department of Industrial Design,
National Institute of Technology,
Rourkela 769008, Odisha, India
Email: rahulkumar589@gmail.com

Saurav Datta* and Manoj Masanta

Department of Mechanical Engineering,
National Institute of Technology,
Rourkela 769008, Odisha, India
Email: sdattaju@gmail.com
Email: manoj.masanta@gmail.com
*Corresponding author

Bibhuti Bhusan Biswal

Department of Industrial Design,
National Institute of Technology,
Rourkela 769008, Odisha, India
Email: bbbiswal@nitrkl.ac.in

Siba Sankar Mahapatra

Department of Mechanical Engineering,
National Institute of Technology,
Rourkela 769008, Odisha, India
Email: ssm@nitrkl.ac.in

Abstract: An experimental investigation has been carried out on electro-discharge machining (EDM) of Inconel 718 using copper electrode tool. Based on L25 orthogonal array, experiments have been conducted by utilising five controllable process parameters (viz. gap voltage, peak current, pulse-on time, duty factor and flushing pressure), each varied at five discrete levels, within selected parametric domain. The following responses in relation to surface characteristics of EDMed Inconel 718, i.e., roughness average (R_a), surface crack density (SCD) and white layer thickness (WLT) have been investigated. SEM micro-graphs revealing various surface irregularities associated in surface morphology of the EDMed Inconel 718 have been analysed in detail and correlated with the information obtained through EDAX, XRD and micro-hardness tests of the machined surface. The presence of different types of cracks within EDMed end product has also been identified. Effects of significant process parameters on surface topography in terms of roughness average, SCD, white layer thickness, etc. have been graphically

represented. Finally, utility theory in conjugation with Taguchi's optimisation philosophy has been attempted to select the most favourable process environment (parameters setting) to satisfy optimal R_a, SCD and WLT; thereby, ensuring high product quality along with its specified functional requirements in appropriate application domain.

Keywords: electro-discharge machining; EDM; Inconel 718; surface crack density; SCD; white layer thickness; WLT; utility theory; Taguchi's optimisation philosophy.

Reference to this paper should be made as follows: Rahul, Datta, S., Masanta, M., Biswal, B.B. and Mahapatra, S.S. (2018) 'Analysis on surface characteristics of electro-discharge machined Inconel 718', *Int. J. Materials and Product Technology*, Vol. 56, Nos. 1/2, pp.135–168.

Biographical notes: Rahul is a PhD Research Scholar in the Department of Industrial Design, National Institute of Technology Rourkela, India. He completed his BTech from JSS Academy of Technical Education, Noida in 2011. He did his MTech in the Department of Mechanical Engineering (specialisation in Welding and Fabrication) from Sant Longowal Institute of Engineering and Technology, Sangrur, Punjab. His area of interest includes non-conventional machining, welding technology, quality optimisation, metal characterisation, cryogenic, modelling and simulation of production processes.

Saurav Datta is currently working as an Assistant Professor in the Department of Mechanical Engineering, National Institute of Technology, Rourkela, India. He obtained his BME and PhD degree from Jadapur University Kolkata in the 2003 and 2008, respectively. His current area of research includes quality optimisation, modelling manufacturing processes, and multi-criteria decision-making. He has published more than 100 papers in various journals of national/international repute; and also published approximately 200 papers in proceedings of various conferences/symposia in India and abroad. He has already produced five PhD with the capacity of Sole Supervisor in NIT Rourkela; and four PhD with the capacity of co-Supervisor in Jadavpur University Kolkata. He has successfully completed one SERB, DST sponsored project on "Machining of CFRP Composites". He is a life member of Indian Institute of Welding (IIW). Currently, he is holding the position of HOD, Central Workshop of NIT Rourkela.

Manoj Masanta is currently working as an Assistant Professor in the Department of Mechanical Engineering, NIT Rourkela. He obtained his PhD in Mechanical Engineering in 2010 from Indian Institute of Technology, Kharagpur. He completed his Bachelor's degree in Production Engineering from Jadavpur University, Kolkata, in 2004 and obtained his Master's degree in Production Technology from the same university in 2006. His present research interests include laser coating, TIG coating, surface engineering, non-conventional manufacturing. He has co-authored several international journals of repute.

Bibhuti Bhusan Biswal is a Professor in the Department of Industrial Design, National Institute of Technology, Rourkela, India. He is currently acting as the Dean (Faculty Welfare) of this institute. He has vast experience in teaching, research and institute administration (as Prof. In-Charge, Training and Placement). His current area of research includes robotics, neural networks, and non-traditional optimisation and simulation.

Siba Sankar Mahapatra is a Professor in the Department of Mechanical Engineering, National Institute of Technology, Rourkela, India. He has more than 20 years of experience in teaching and research. His current area of research includes multi-criteria decision-making, quality engineering, assembly line balancing, group technology, neural networks, and non-traditional optimisation and simulation. He has published more than 40 journal papers. He has written few books related to his research work. He is currently dealing with few sponsored projects.

1 Research background

Inconel 718 belongs to the category of heat-resistant super alloys (also called high-temperature alloys) which possess high temperature corrosion resistance, oxidation resistance, and creep resistance. Because of these characteristics, this super alloy is widely applied in components of aircraft engines and industrial gas turbines. It is also used in petrochemical, oil, and biomedical applications, specifically owing to their excellent corrosion resistance.

Inconel 718 exhibits poor machinability. The unique characteristic i.e., excellent high-temperature strength makes it 'difficult-to-cut'. The main challenges towards machining of Inconel 718 include: (source: http://www.kennametal.com).

- While machining, the high strength of Inconel 718 at hoisted cutting temperatures causes high cutting forces; which in turn, generates enormous heat at the tool tip and limits cutting speed considerably.
- The low thermal conductivity of Inconel 718 is responsible for transferring huge amount of heat generated during machining to the tool, subsequently increasing tool-tip temperature and promoting excessive tool wear (mainly crater wear) and severe plastic deformation of the cutting tool edge. These phenomena can limit cutting speeds and can reduce tool life.
- The presence of hard abrasive intermetallic compounds and carbide particles in these alloys may cause severe abrasive wear on the tool tip, thereby reduce tool life.
- The chemical reactivity of Inconel 718 stimulates formation of Built Up Edge (BUE) and coating delamination, which appears detrimental for tool life.
- The work-hardening property of Inconel 718 incurs depth-of-cut notching on the tool, leading to burr formation on the work surface. Tough and continuous chips are formed which necessitate efficient chip breaker geometry.
- Enormous heat during machining can alter microstructure of the work material. Induced residual stress can affect fatigue life of the part component adversely.

Compared to conventional operations, non-conventional machining is experienced as advantageous for Inconel 718 to transform into desired shape and size with intricate geometry and required dimensional accuracy.

Literature depicts that considerable volume of work has been attempted by previous researchers on machining and machinability aspects of Inconel 718. Ramakrishnan and Karunamoorthy (2008) developed artificial neural network (ANN) models and attempted for multi-response optimisation to predict and select the best process environment of wire electro-discharge machining (WEDM) for Inconel 718. Experiments were performed under different cutting conditions of pulse-on time, delay time, wire feed speed, and ignition current. The WEDM responses were optimised concurrently using multi-response signal-to-noise (MRSN) ratio in addition to Taguchi's parametric design approach. Newton et al. (2009) conducted an experimental investigation to determine the main EDM parameters contributing to recast layer formation in Inconel 718. It was found that average recast layer thickness increased primarily with energy per spark, peak discharge current, and pulse duration. Kumar et al. (2011) studied the influence of process parameters on machining characteristics of Inconel 718 in aluminium additive mixed electric discharge machining (AEDM) with copper electrode. The effectiveness of AEDM process on Inconel was evaluated in terms of material removal rate, surface roughness, and wear ratio. It was concluded that particle concentration and its size significantly affected machining efficiency.

Rajesha et al. (2012) experimented on EDM process for machining of Inconel 718 using a copper electrode tool having tubular cross-section. Experiments were planned using response surface methodology (RSM). Effects of five major process parameters (pulse current, duty factor, sensitivity control, gap control, and flushing pressure) on two process responses (material removal rate and average roughness of EDMed work surface) were discussed in this paper. Experiments revealed that the thickness of the sputtered layer and the crack length were found to be highly influenced by pulse current. Lin et al. (2013) applied Grey-Taguchi method for optimisation of micro-milling electrical discharge machining process parameters of Inconel 718 to achieve multiple performance characteristics such as low electrode wear, high material removal rate and low working gap. The influences of peak current, pulse on-time, pulse off-time and spark gap on aforesaid machining responses were also analysed. Ay et al. (2013) applied grey relational analysis (GRA) method to optimise micro-electrical discharge drilling process of Inconel 718 with multi-performance characteristics i.e., hole taper ratio and hole dilation. As compared to pulse duration, pulse current was found to be more significant on influencing machining performance.

Dhanabalan et al. (2014) investigated on EDM of Inconel 718 and Inconel 625 super alloys. The significance of input parameters namely peak current, pulse-on time, and pulse-off time on form-tolerances was investigated. Prihandana et al. (2014) investigated the influence of molybdenum disulfide (MoS_2) powder suspended in dielectric fluid on the performance of micro-EDM of Inconel 718 with focus in obtaining quality micro-holes. Li et al. (2015) focused on machining characteristics of Inconel 718 by wire-EDM and sinking-EDM with a Cu-SiC electrode, respectively. Material removal efficiency, surface roughness, surface topography, surface alloying, and electrode wear etc. were investigated in this work. It was claimed that high toughness of Inconel 718 would be the major contributing factor to the absence of micro-cracks on the EDMed surface. The fabricated Cu-SiC electrode for sinking-EDM showed better performance in terms of material removal rate, surface roughness, and electrode wear. Aggarwal et al. (2015) explored RSM towards empirical modelling of process parameters of the WEDM for Inconel 718. The parameters such as pulse-on time, pulse-off time, peak current, spark gap voltage, wire feed rate, and wire tension were selected as input variables;

whilst, the overall performance was measured in terms of cutting rate and surface roughness.

Owing to the widespread application of Inconel 718 especially over automotive, aerospace and defence industries; machining and machinability aspects of this super alloy has become an important research agenda today. However, machining of Inconel seems a challenge since several difficulties are likely to arise due to their high strength, high temperature resistance, work-hardening tendency, affinity to form built-up edge etc.; which restricts processing of Inconel 718 through conventional machining operations. On the contrary, non-conventional machining processes like EDM, ECM, wire-EDM routes etc. have been recommended by part researchers to improve machining performance on Inconel 718 and consequently satisfactory product quality up to the desired extent. In this context, an attempt has been made to investigate different aspects of EDM of Inconel 718 using Cu tool electrode.

EDM process is controlled by several input parameters: gap voltage, peak discharge current, pulse-on duration, pulse-off duration, duty factor, flushing pressure etc. Peak current can be defined as the maximum value of discharge current intensity applied between tool electrode and the workpiece to be machined by EDM. As described by Jabbaripour et al. (2012), pulse-on time is the period in which the current is allowed to flow per cycle. Open circuit voltage (OCV) is the potential difference between tool and workpiece before pulse generation. The duty factor is the ratio of pulse-on time relative to total cycle time. The flushing pressure is the pressure at which flushing is done by forcing the dielectric fluid through the inter electrode gap so that debris can be transported away from the machining zone. Otherwise, the EDM debris or chips tend to be re-machined again and again, obstructing the machining process to progress effectively [Source: www.EDMtodayMagazine.com]. Literature depicts that EDM input parameters interact in a complex manner, thereby, affecting process performance characterises [material removal rate, tool wear ratio, roughness average (R_a), surface crack density (SCD), white layer thickness (WLT), etc.]. Critical analysis is indeed required to control EDM response features before the part component is subjected to service. In this context, in-depth understanding on formation of surface cracks as well as while layer is highly essential to suppress the occurrence of those and to minimise detrimental effects imposed by them.

Crack formation in EDMed component is incurred due to presence of thermal stress and tensile stress within the machined surface. As explained by Guu and Hou (2007), thermal stress is evolved due to drastic heating and subsequent cooling of the machined zone and the consequence of uneven temperature distribution. Tensile residual stress within the specimen is generated because dielectric is incapable of washing out the debris completely from the machined zone. Yan et al. (2005), Ekmekci et al. (2006) and Ekmekci (2007) explained that due to the ingress of carbon particles either from electrode or from pyrolysis of dielectric fluid (hydrocarbon), the molten material contracts to a greater extent as compared to unaffected parent part during the cooling process; and, when the stress in the surface rises above the material's ultimate tensile strength, cracks are formed.

During EDM operations, existence of recast or white layer (WL) is highly undesirable, but its formation is inevitable. Hence, as pointed out by Yildiz et al. (2015), the mechanism behind WL formation needs to be clearly understood and its thickness should be accurately determined to efficiently perform post-treatment operations for removing the WL resulted by the EDM process.

At the end of each discharge, depending on the plasma flushing efficiency (%PFE) (i.e., the ability of plasma channel in removing molten material from the molten material crater), collapsing of plasma channel causes violent suction and severe bulk boiling of some molten material and removal of them from the molten crater. The material remained in the crater re-solidifies, which is called the 'WL' or 'recast layer'. An annealed heat affected zone (HAZ) lay directly below the recast layer. The micro-cracks created in the WL can penetrate into the HAZ. Additionally, this layer appears softer than the underlying base material. This annealed zone is prematurely weak; and cause fracture that can lead to minor malfunctioning of the part and finally catastrophic failure.

The melting and re-solidification of the material causes formation of WL onto the top of the machined surface. Rao et al. (2008) described that the formation of WL and HAZ adversely affect surface integrity (which is characterised by high surface roughness i.e., R_a value), development of residual stress, altered composition of the surface, reduced corrosion resistance etc. Therefore, formation of while layer and HAZ needs to be controlled.

It is understood that different response features during EDM correspond to conflicting requirements in the sense that high MRR is strongly appreciated whereas, attention must be paid to ensure minimal tool wear, R_a, SCD as well as WLT. Proper control of process input parameters may achieve satisfactory machining performance. Hence, it is customary to understand the effect of process variables on various response measures of EDM process. In earlier literature, emphasis has been made to investigate effect of electrical parameters (mainly discharge current, pulse duration and duty factor) on various performance measures; little attempt has been made to examine the effect of flushing pressure on aforementioned responses in the context of EDM on Inconel 718. Apart from this, literature is sparse in correlating machining responses like R_a, SCD and WLT with micro-hardness and residual stress resulted with EDMed workpiece along with its change in chemical composition and metallurgical aspects like phases present, grain orientation etc. The present study has been aimed to examine these aspects through experimentation and subsequent data analysis.

An unique attempt has also been made to optimise different performance measures in relation to surface topography of the EDMed Inconel 718 viz. R_a, SCD and WLT simultaneously; thus, to determine the most favourable process environment (parameters setting). Utility-based Taguchi approach has been attempted in this part of work.

Figure 1 Copper electrode (see online version for colours)

2 Experimental details

Inconel 718 plates of dimension (50 × 50 × 5) mm^3 have been used as work material. The chemical composition and mechanical properties of Inconel 718 have been depicted in Table 1a and Table 1b, respectively. A pure (99.9%) copper rod of circular cross-section has been used as tool electrode (Figure 1).

Table 1a Chemical composition of Inconel 718

Element	*Range (% wt.)*
Ni	50.50
Fe	20.24
Cr	18.16
Nb	5.02
Mo	2.91
Ti	1.05
Al	0.62
Co	0.15
Si	0.08
Mn	0.07
Cu	0.06
C	0.05
P	0.008
Ta	0.003
B	0.003

Table 1b Properties of Inconel 718

Property	*Value*
Density	8.19 g/cm^3
Thermal conductivity	11.2 W/m-K
Electrical resistivity	127 μΩ cm
Elastic modulus	200 GPa
Yield strength	434 GPa
Tensile strength	855 MPa
Hardness	89 HRB

The experiments have been carried out on die sinking EDM setup (make: Electronica ElektraPlusPS 50ZNC, India). Commercial grade EDM oil (with specific gravity of 0.763 and flushing point 94°C) has been used as dielectric fluid. Polarity has been kept positive (i.e., workpiece positive). The other parameters such as gap servo sensitivity (SEN), anti-arcing sensitivity (ASEN), working time (Tw), and lift time (T″) have been kept at constant values (refer to Table 2) through entire experimentation.

Table 2 Fixed/constant parameters

SEN	*ASEN*	*Tw (s)*	*T↑ (s)*	*Pol*
6	3	0.3	0.2	+ve

Table 3 Machining control parameters: domain of variation

Parameters	*Unit*	*Notation*	*Levels of variation*				
			1	*2*	*3*	*4*	*5*
Gap voltage (V_g)	[V]	A	50	60	70	80	90
Peak current (I_P)	[A]	B	3	5	7	9	11
Pulse-on-time (T_{on})	[μs]	C	100	200	300	400	500
Duty factor (τ)	[%]	D	65	70	75	80	85
Flushing pressure (F_p)	[bar]	E	0.2	0.3	0.4	0.5	0.6

Table 4 Design of experiment (L25 OA) and collected experimental data

Sl. no.	*L25 OA (factors are in coded form)*					*Experimental data*			
						Response variables to be optimised simultaneously			*MH [HV0.05]*
	A	*B*	*C*	*D*	*E*	*Ra [μm]*	*SCD [μm/μm2]*	*WLT [μm]*	
1	1	1	1	1	1	3.800	0.0158	19.261	439.3333
2	1	2	2	2	2	6.333	0.0166	19.577	387.7000
3	1	3	3	3	3	9.133	0.0151	16.954	441.1333
4	1	4	4	4	4	9.867	0.0136	18.596	463.7000
5	1	5	5	5	5	7.600	0.0141	17.667	389.5667
6	2	1	2	3	4	3.733	0.0154	19.074	391.4333
7	2	2	3	4	5	4.400	0.0152	17.065	518.0667
8	2	3	4	5	1	8.067	0.0152	17.523	388.9667
9	2	4	5	1	2	7.667	0.0156	20.308	373.8667
10	2	5	1	2	3	9.600	0.0056	17.742	392.4333
11	3	1	3	5	2	2.967	0.0189	19.861	394.5000
12	3	2	4	1	3	5.533	0.0163	20.090	390.0000
13	3	3	5	2	4	7.267	0.0168	20.100	406.4333
14	3	4	1	3	5	8.533	0.0093	19.445	405.9667
15	3	5	2	4	1	9.733	0.0125	19.086	390.3000
16	4	1	4	2	5	4.267	0.0172	18.310	384.1333
17	4	2	5	3	1	5.267	0.0157	18.067	352.6000
18	4	3	1	4	2	7.200	0.0108	18.137	385.6333
19	4	4	2	5	3	5.667	0.0084	18.673	390.6333
20	4	5	3	1	4	9.867	0.0110	18.835	410.7333
21	5	1	5	4	3	2.133	0.0156	17.602	378.2000
22	5	2	1	5	4	5.667	0.0117	16.646	372.9000
23	5	3	2	1	5	7.333	0.0136	17.707	375.8000
24	5	4	3	2	1	9.200	0.0116	19.752	399.1000
25	5	5	4	3	2	10.333	0.0100	19.077	431.8667

In the present work, five controllable process variables (parameters) have been selected based on literature survey. The selected process parameters have been OCV (also called gap voltage; V_g), peak current (I_p), pulse-on time (T_{on}), duty factor (τ) and flushing pressure (F_p). As per present experimental layout, each process parameter under consideration has been varied at five discrete levels (Table 3), as per provision of parametric setting (adjustment) available with the setup. The design of experiment has been selected based on five-level-five-factor L_{25} orthogonal array (OA) (Table 4).

Experiments have been conducted as per 25 factorial settings; the EDM of Inconel 718 plates have been carried out with copper electrode. Both workpiece and tool have been immersed in dielectric fluid. The machining duration has been kept constant (ten minutes) for each experimental run. After performing experiments, in order to analyse surface characteristics of EDMed Inconel 718, the responses studied herein have been R_a, SCD and WLT of the EDMed specimen.

In addition to that, the micro-hardness of WLs for all EDMed specimens has been determined by Vicker's micro-hardness tester (make: LECO, USA; Modal No. LM810). Hardness measurements have been carried out with test load of 50gf and at a constant indenter dwell time of 10s. All indentation tests have been carried out under ambient laboratory conditions.

In order to determine the elements and phases present on the surface of as received Inconel 718 as well as EDMed Inconel 718 specimen, EDS (energy dispersive spectrograph) and XRD (X-ray diffraction) have been carried out. In this work, the chemical compositions of Inconel 718 before and after machining have also been detected by energy dispersive X-ray spectroscopy (EDAX or EDS) under Scanning Electron Microscope (model No. SU3500) with EDAX (Model No. 51_ADD0034), manufactured by Hitachi, Japan.

The phases present on EDMed surface of Inconel 718 along with residual stress induced within the part component have been determined by X-ray diffraction microscopy (model no: D8 ADVANCE with DAVINCI design, Make: BRUKER, Germany). Apart from Inconel 718 (as received), residual stress induced within EDMed specimen produced at Run No. 1 i.e., (V_g = 50 V; I_P = 3 A; T_{on} = 100 μs; τ = 65%; F_P = 0.2 bar) has been measured and compared with each other. In addition to these, XRD spectra for the surface of as received Inconel 718 as well as EDMed Inconel 718 (obtained at run no. 1) have been analysed to identify various phases present therein along with to collect the information in relation to grain refinement, alloying effect, formation of new phase etc. as the consequences of EDM operations. There has been analysed in the following sections.

The experimental results in relation to process responses like R_a, SCD and WLT have been depicted in Table 4. The snapshot of EDM machined workpieces has been provided in Figure 2. Definitions of aforesaid response measures in the context of the present work have been provided below.

Figure 2 EDM machined workpiece of Inconel 718 (see online version for colours)

2.1 Surface roughness

Arithmetic average roughness, or R_a, is the arithmetic average of the heights of surface irregularities (consisting of peak heights and valleys) with respect to the mean line, measured within the sampling length. The measurement of surface roughness (R_a value) of the EDMed surface has been carried out with portable stylus type profilometer, Talysurf (model: Taylor Hobson, Surtronic 3+), with cut-off length (L_c) of 0.8 mm, sample length (L_n) of 4 mm, and filter CR ISO.

2.2 SCD

It is well known that generation of surface crack is detrimental since it results inferior surface finish. It seems very difficult to quantify the phenomenon cracking in terms of width, length, or depth of the crack or even by the extent of cracking; therefore, in the present work, SCD has been measured and analysed to evaluate the severity of cracking. As mentioned by Bhattacharyya et al. (2007), SCD is defined as the total length of cracks (μm) per unit surface area (μm^2).

In course of the present work, to measure SCD, the top surface morphology of the EDMed Inconel 718 specimen has been studied using scanning electron microscopy (SEM). For a particular sample, SEM images have been captured in three distinct locations and corresponding surface crack densities have been collected. The average of these three has been considered as the representative measure of SCD for that particular specimen. For a particular sample area, the total crack length has been measured using PDF-X Change Viewer Software. The total crack length divided by the specimen area provided the measure of SCD.

2.3 WLT

In order to measure WLT, each specimen has been sectioned in appropriate dimension and cold mounted by using cold mounting compound resin bed revealing the edge of the

workpiece to go for polishing operation. For cold mounting of specimens, Geosyn cold mounting compound powder and liquid have been used. The cold mounted specimens have been polished successively on water-proof SiC papers with grit sizes 120, 320, 400, 600, 800, 1,200 and 1,500, respectively. Grinding with each paper has been performed for 60–120 seconds at 240–300 RPM speed of the grinding wheel. Finally, the specimen surface has been polished with SELVYT Cloth (made in England) and diamond paste of 1 μm size. The surface has then been subsequently electro-polished with slurry of HIFIN Fluid with 'OS' type diamond compound. Next, the polished surface has been etched in Kalling's Reagent solution (5 g $CuCl_2$ + 100 ml conc. HCl + 100 ml pure ethanol) for 20s immersion. This has been felt necessary in order to expose WL and corresponding distinct boundary line separating HAZ and/or base metal. The specimen has then been viewed under SEM (model, Joel JSM-6480LV, Japan) to capture the image of WL formed. The thickness of the WL has been measured by ImageJ Software at five different locations across each cross-sectioned specimen; and an average value has been considered for further analysis.

3 Data analysis

3.1 Analysis of SEM micrographs: results of EDAX, XRD and micro-hardness tests

As compared to the unaffected parent material (Figure 3), the EDMed surface of Inconel 718 observed under SEM reveals existence of irregular topography which consists of several defects including overlapping craters, globules of debris (special deposition), pockmarks or 'chimneys' [Figures 4(a) to 4(b)].

Figure 3 SEM images of Inconel 718, (a) surface structure (before machining) (b) (a) surface structure (after machining) (sample no. 1) (see online version for colours)

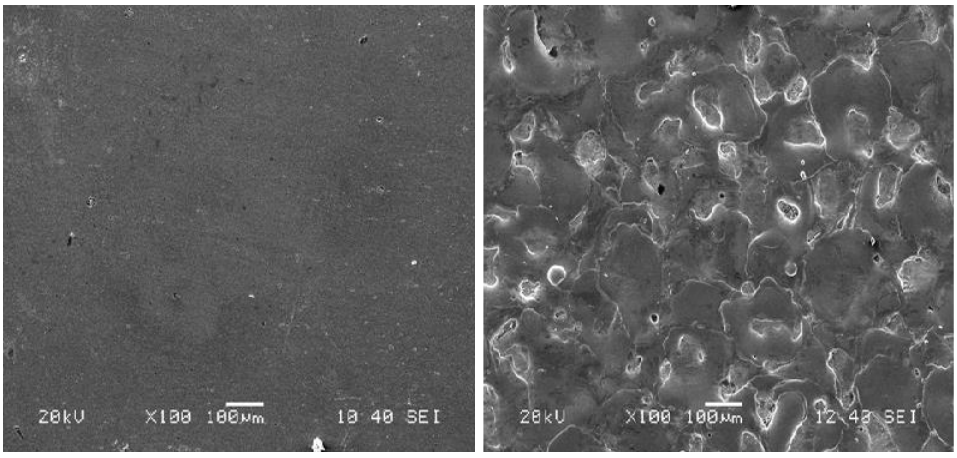

(a) (b)

Figure 4 (a) Surface morphology of EDMed Inconel 718 performed on parametric setting (V_g = 50 V; I_P = 9 A; T_{on} = 400 µs; τ = 80%; F_P = 0.5 bar) (b) Surface morphology of EDMed Inconel 718 performed on parametric setting (V_g = 80 V; I_P = 11 A; T_{on} = 300 µs; τ = 65%; F_P = 0.5 bar) (see online version for colours)

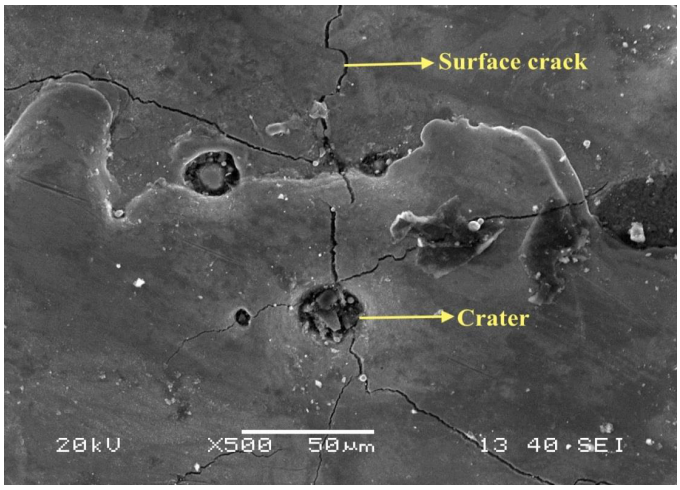

(a)

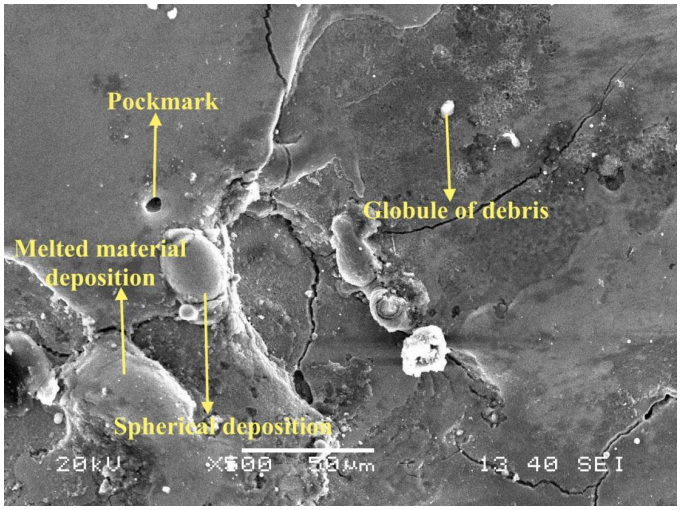

(b)

Another prominent feature that has been found in on the machined surface is the existence of micro-cracks in abundance [Figures 4(a) to 4(b)]. The spherical shape has been resulted from the effect of surface tension. Pockmarks have been generated on the surface due to gas bubbles expelled from the molten material during solidification. The micro-cracks have been found due to the consequence of thermal stresses developed.

Figure 5 SEM image revealing existence of WL and HAZ as observed in EDMed Inconel 718 at (V_g = 70 V; I_P = 5 A; T_{on} = 400 µs; τ = 65%; F_P = 0.4 bar) (run no. 12) (see online version for colours)

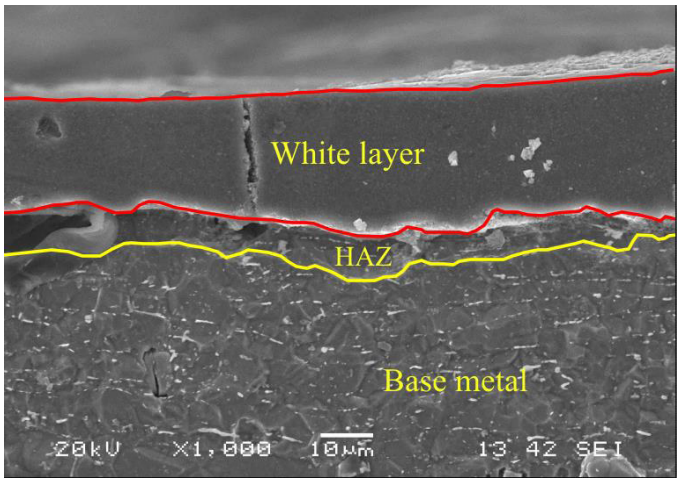

Typically the finished EDMed workpiece exhibits several distinct layers (Figure 5). On the top surface, formation of WL is responsible for altering metallurgical structure of the workpiece. According to Tsai et al. (2003), it is quite hard and non-etchable. Next to WL, heat-affected zone (HAZ) or annealed layer appears. This layer is heated during operation but not melted. This layer experiences high temperature rise to cause a quenching effect. It is also referred to as the 'rehardened layer'. Newton et al. (2009) explained that the HAZ contains an altered microstructure, tensile stresses, micro-cracks, impurities, and other undesirable features which can lead to premature part failure whilst subjected to service.

Ekmekci (2009) reported that cracks developed on EDMed work piece have three distinctive characteristics. The first type of micro-cracks, called surface cracks, appears in the WL which initiates at its surface and tends to propagate perpendicularly down toward the interferential zone, separating the HAZ and the WL, and usually terminates at this interference. The second type of micro-cracks, denoted as penetrating cracks, penetrates the entire WLT with a tendency to emerge into the parent material. The third type of micro-cracks can be identified to be present usually around globular or irregular-shaped attachments on crater rims. Such cracks correspond to negligible depth of penetration and are randomly distributed over the EDMed surface. However, analysis of SEM micrographs of EDMed specimens could retrieve only two crack types (first and third type) distinctly [Figures 6(a) to 6(b)].

This can be attributed by the fact that the parametric settings employed herein might not be enough to reveal development of cracks of second type. Since surface cracking is the combined effect of induced residual stress along with thermal stress developed during EDM operations. Evolution of such stresses and their magnitude highly depends on the process environment (parameters setting) employed. Since the process parameters influence the machining performance to a varied degree (levels of significance are different), variation of parametric settings incur surface cracking with varied intensity.

Figure 6 (a) Existence of crack (type 1) as observed in EDMed Inconel 718 performed on parametric setting (V_g = 70 V; I_P = 7 A; T_{on} = 500 µs; τ = 70%; F_P = 0.5 bar) (run no. 13) (b) Existence of crack (type 3) as observed in EDMed Inconel 718 performed on parametric setting (V_g = 80 V; I_P = 11 A; T_{on} = 300 µs; τ = 65%; F_P = 0.5 bar) (run no. 20)

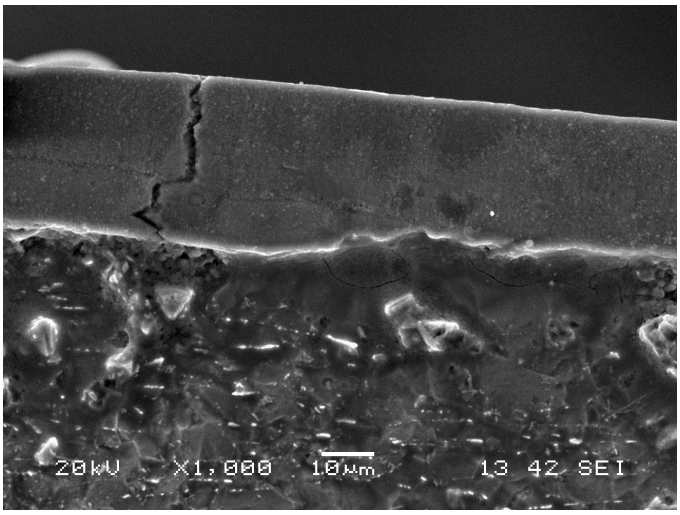

(a)

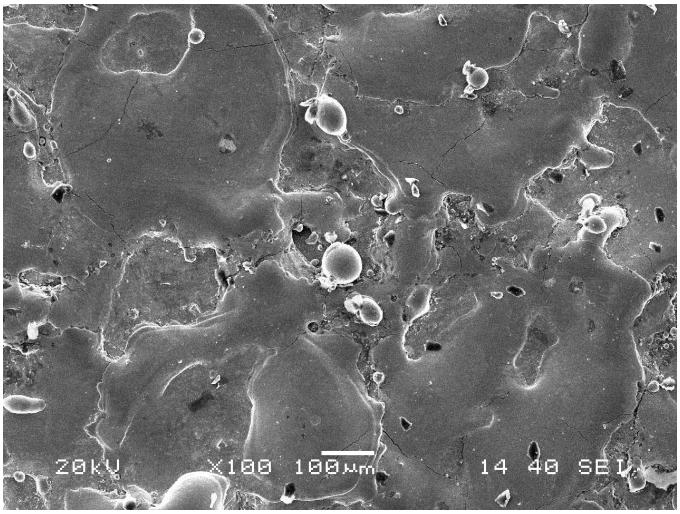

(b)

According to Opitz (1960), WL is generally heavily alloyed with the pyrolysis products from the cracked dielectric fluid as well as tool electrode and thus possesses high hardness values; however distribution of micro-hardness seems non-uniform with respect to EDM parameters settings. This has also been reflected by the EDAX analysis of EDMed Inconel 718 with respect to the as received Inconel 718.

Figure 7 (a) Chemical composition of Inconel 718 (as received) retrieved from EDAX analysis (b) Chemical composition of EDMed Inconel 718 as retrieved from EDAX analysis with parameters setting (V_g = 50 V; I_P = 3 A; T_{on} = 100 µs; τ = 65%; F_P = 0.2 bar) (run no. 1) (c) Chemical composition of EDMed Inconel 718 as retrieved from EDAX analysis with parameters setting (V_g = 90 V; I_P = 11 A; T_{on} = 400 µs; τ = 75%; F_P = 0.3 bar) (run no. 25) (see online version for colours)

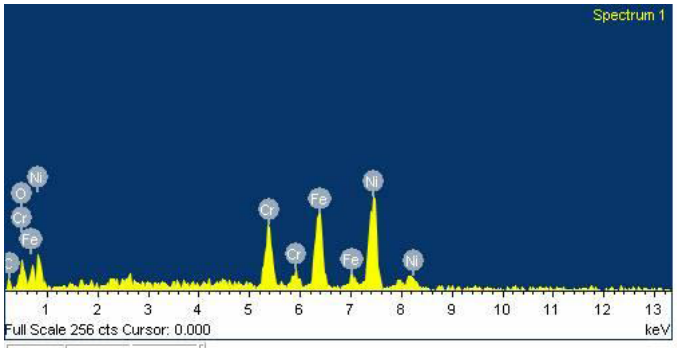

Element	Weight%	Atomic%
C K	10.43	30.40
O K	9.10	19.90
Cr K	12.83	8.63
Fe K	24.92	15.62
Ni K	42.71	25.45
Totals	100.00	

(a)

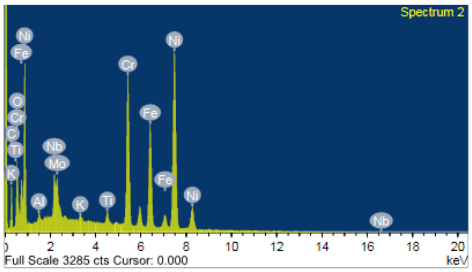

Elem...	Weight%	Atomic%
C K	22.19	51.62
O K	8.71	15.22
Al K	0.37	0.38
K K	0.22	0.16
Ti K	0.74	0.43
Cr K	13.45	7.23
Fe K	12.79	6.40
Ni K	34.76	16.54
Nb L	4.17	1.25
Mo L	2.60	0.76
Totals	100.00	

(b)

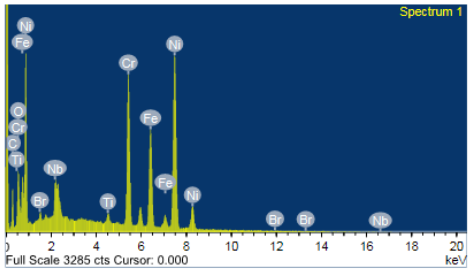

Elem...	Weight%	Atomic%
C K	16.28	43.46
O K	6.90	13.82
Ti K	0.75	0.50
Cr K	15.91	9.81
Fe K	14.63	8.40
Ni K	40.92	22.35
Br L	1.14	0.46
Nb L	3.48	1.20
Totals	100.00	

(c)

By comparing Figures 7(b) to 7(c) with respect to Figure 7(a), it has been observed that carbon content of Inconel 718 has been increased during EDM operation. It has been noted that wt% of C in Inconel 718 has been substantially increased from (10.43 wt% C, for as received Inconel 718) to 22.19 wt% (for EDMed specimen prepared at run no. 1) and 16.28 wt% (for EDMed specimen prepared at run no. 25). This has resulted higher hardness value of EDMed Inconel 718 as compared to the base material. The micro-hardness values acquired at the top machined surface of Inconel 718 have been computed for all experimental runs and depicted in Table 4. It has been observed that it varies from 352.600 $HV_{0.05}$ to 518.067 $HV_{0.05}$ for the EDMed specimens prepared under different parameters settings; whereas, micro-hardness of Inconel 718 (as received) corresponds to a hardness value of 269.400 $HV_{0.05}$. Increased micro-hardness of the machined surface (as compared to base material) is due to carbon enrichment through dielectric cracking. Literature by Tönshoff and Brinksmeier (1980) ascertains that investigation on micro-hardness of EDMed surface is necessary for identifying yield strength changes, structure alterations, work hardening or softening of surface layers, etc. Crookall and Khor (1975) also reported that the hardness of WL appeared to be substantially higher than for the parent material. Guu and Hou (2007) observed non-uniform distribution of micro-hardness in the EDMed part caused by the non-uniformity of micro-structure and chemical compositions in the machined regions. (Ekmekci et al., 2005) experimentally found that the hardness values remain more of less constant within WL. Remarkable decrement in micro-hardness may be observed within HAZ with a tendency to settle down to the unaffected parent material hardness.

Another important aspect of EDM process is the evolution of residual stress within the machined part. Since it plays an important role towards evaluating fatigue life of any machined component. Ogata and Mukoyama (1991), Kruth and Bleys (2000) reported that the EDMed surface exhibits large in-plane tensile residual stresses. Existing literature by Rebelo et al. (1998) depicts that as energy per spark increases, the depth of the peak tensile residual stress also increases. This may be due to the fact that presence of micro-cracks relieves the tensile stress on the surface. The evolution of residual stress can also be explained due to thermal gradients during cooling of the WL. As WL resolidifies and its temperature drops down to that of the bulk workpiece (unaffected parent material), its contraction is opposed by the bulk workpiece. Ekmekci et al. (2005) experimentally found that the residual stress generally increases from the bulk material to a maximum extent and then tends to decrease again near to the surface. This decrease can be logically correlated with occurrences of crack since residual stresses exceeds the fracture strength of the material.

In the present work, XRD analysis reveals that induced residual stress in tensile in nature, for the EDMed Inconel 718 specimen (obtained at run no.1), which corresponds to a value 1.7123 ± 0.268 GPa; which seems substantially higher as compared to the residual stress within as received Inconel 718 i.e., $-(0.4384 \pm 0.127)$ GPa (compressive stress, in the present case).

Tönshoff and Brinksmeier (1980) described that residual stress generated during EDM process is primarily due to non-homogeneity of heat flow and metallurgical transformations or due to localised inhomogeneous plastic deformation, respectively. Moreover, static and dynamic strength, stress corrosion resistance, chemical resistance, and magnetic properties etc. of the EDMed component are influenced by the presence of residual stress. According to Guu and Hocheng (2001) high value of pulse current results

more frequent cracking of the dielectric, thereby, causing more melt expulsions and larger tensile residual stresses. These problems in an amplified manner incur poor surface finish and serious surface damage.

Analysis of X-ray diffraction for unaffected (as received) and EDMed surface of Inconel 718 has been shown in Figure 8.

Figure 8 XRD spectra of as received Inconel 718, and machined surface at run no. 1 i.e., (V_g = 50 V; I_P = 3 A; T_{on} = 100 µs; τ = 65%; F_P = 0.2 bar) (see online version for colours)

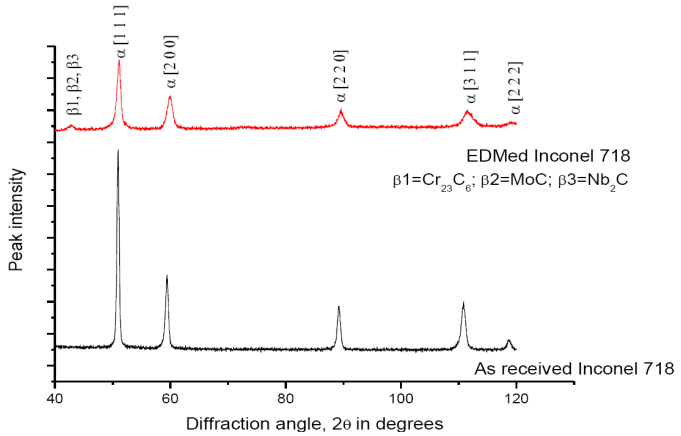

XRD has been performed for determination of any metallurgical changes taking place such as phase transformation or any modification in grain size along with orientation. Crystal structure and phase change phenomenon can be understood by examining the position of the peaks, whereas the crystallite size can be deter-mined through FWHM (full width half maxima). XRD analysis revealed cubic FCC structure of as received Inconel 718 which is basically Ni-based solid solution having PDF index name: chromium cobalt molybdenum nickel (Ni-Cr-Co-Mo) [reference code: 35-1489].

The XRD patterns of the test sample EDMed at Run No.1 (V_g = 50 V; I_P = 3 A; T_{on} = 100 µs; τ = 65%; F_P = 0.2 bar) shows almost similar sequence of peaks. Therefore, it can be concluded that no phase change has incurred during the EDM operation utilising parameters setting of run no. 1. Broadening (FWHM) of peaks on the XRD spectra divulges the variation of the crystallite size. Comparing the XRD spectra of the Inconel 718 (as received) to that of machined surface obtained using run no. 1, clear difference in terms of the intensity and the width of the peaks could be retrieved. Therefore, it can be concluded that EDM process has induced grain refinement of the machined surface. The grain refinement is mainly due to the thermo-mechanical effect which in turn causes metallurgical alteration of the work surface.

XRD pattern of EDMed specimen has revealed existence of an extra peak which may be due to the precipitation of $Cr_{23}C_6$ (chromium carbide), MoC (molybdenum carbide) and Nb_2C (niobium carbide) on the main matrix. This is because, EDM process results carbon enrichment onto the machined zone during pyrolysis of dielectrics. Carbides are thus formed and precipitates on the work surface.

3.2 Study of parametric influence

Literature is rich in establishing and explaining relationships amongst various process parameters with respect to different EDM responses. Most of the earlier studies concentrated on understanding the influence of electrical parameters (spark gap voltage, gap voltage, discharge current, pulse-on time, pulse-off time, duty factor) on different machining responses. Rare attempt has been made to reveal the effect of flushing rate on EDM performances on Inconel 718. Flushing plays an important role during EDM operations and the rate at which it takes place should be properly adjusted so as to improve overall machining yield.

Wong et al. (1995) stated that the dielectric fluid applied for EDM should possess high dielectric strength and ability to quick recovery after breakdown, effective quenching and flushing capability. During EDM flushing, the dielectric fluid is distributed through the spark gap in order to remove debris (eroded particles) generated during EDM and to maintain dielectric temperature well below its flash point. Hence, it seems necessary to study the effect of flushing rate on different features of machining performance during EDM of Inconel 718. Improper flushing may result in uneven tool wear, affecting machining accuracy and poor surface finish; it can also reduce material removal rate due to unstable machining environments and arcing around regions with high concentration of debris.

In this part of work, research has been extended to identify the effect of various electrical parameters (especially I_p, T_{on} and τ) along with dielectric flushing circulation pressure on surface roughness, SCD and WLT of the EDMed end product. Experimental data corresponding to L_{25} OA design seems insufficient to reflect accurate trend of variation of output response(s) with respect to process inputs; Taguchi method has been explored to generate required number of response data with respect to all possible parametric combinations as per full factorial experimental design. Taguchi predicted response data have been plotted to exhibit the direct effect of process parameters on R_a, SCD, and WLT for EDMed Inconel 718; trends of variations thus observed have been compared to that of reported in literature for other materials within specific domains of experiments. However, these tends shown herein are approximated ones since Taguchi method assumes linear relationship of the output(s) with respect to the inputs; however, in practice, this may not be so. Hence, two successive points on the direct effect plots have been joined by means of a straight line rather than a smooth cure.

3.2.1 Parametric influence on surface roughness

According to Lee and Yur (2000), it is understood that the performance and service life of EDMed end product is greatly influenced by the surface characteristics developed during surface erosion. Proper tuning of controllable process parameters may yield satisfactory machining performance in terms of surface finish. Hence, adequate knowledge about the influence of process parameters on surface roughness is of utmost important.

Figure 9 Effect of peak current (B) on R_a (see online version for colours)

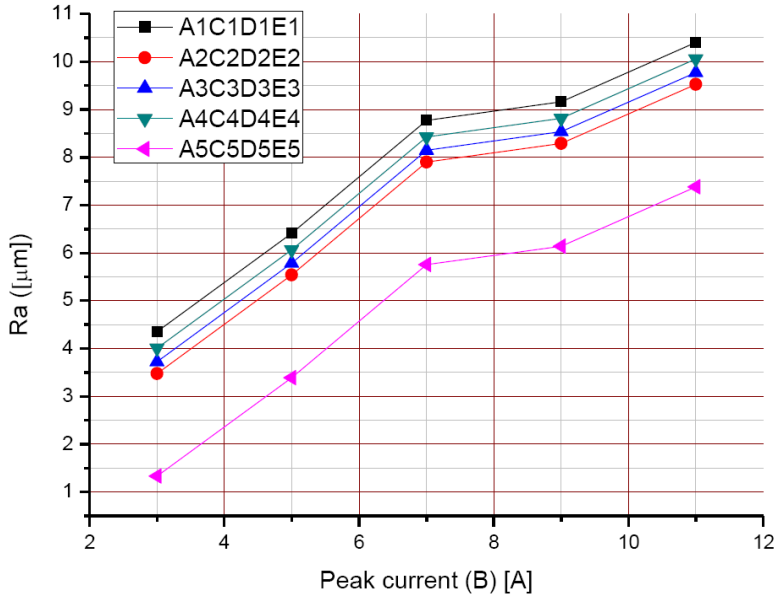

The effect of peak current (B) on surface roughness (R_a) has been presented graphically in Figure 9. It has been observed that surface roughness tends to increase as peak current increases, while keeping other parameters fixed at constant levels. This can be attributed by the fact that as peak current increases; discharges strike the specimen surface more intensely, which in turn results enormous erosion effect, thereby, causing deterioration of the surface morphology to a remarkable extent. Rajesha et al. (2010) explained that the higher input power associated with increased pulse current causes huge distortion on the EDMed surface due to more frequent molten material expulsion. This leads to an increase in R_a value.

Guu et al. (2005), Ramasawmy et al. (2005) and Keskin et al. (2006) found that that superior surface finish can be achieved by adjusting process control parameters at a low pulse current and a small pulse-on time. According to Simao et al. (2003), low values of R_a can only be obtained with low levels of discharge energy. Hewidy et al. (2005) and Williams and Rajurkar (1991) reported that surface roughness increases with increased peak discharge current.

Huang et al. (1999) and Hasçalýk and Çaydaş (2004) also claimed that surface roughness increases with increase in energy per spark during EDM operations.

The effect of pulse-on time (C) of R_a has been plotted in Figure 10. It has been observed that while keeping other parameters fixed at constant level values; an increase in T_{on} (up to 400μs) results increase in R_a. Increase in T_{on} produces adverse effect on the workpiece by increasing surface roughness. Similar trend has also been observed by Lee and Tai (2003). It may be due to the fact that for T_{on} (in between 100–400 μs), deeper

discharge craters are expected to be formed and more material is eroded per spark since spark energy is directly proportional to T_{on}. This leads to increase in R_a values. For the values of T_{on} (beyond 400µs) the drop in R_a can be understood by high values of pulse-off time. Since duty factor has been kept fixed at contest level, a higher T_{off} value has been allowed corresponding to a higher T_{on} value. However, no material removal is incurred during T_{off}. The T_{off} being sufficiently large the total machining time increases, which in turn decreases MRR as well as R_a. However, Saha and Choudhury (2009) reported that this non-cutting time does not have a significant effect on the R_a value. Huang et al. (1999) and Ramakrishnan and Karunamoorthy (2008) also experimentally examined that surface roughness increases with increased pulse duration.

Figure 10 Effect of pulse-on time (C) on R_a (see online version for colours)

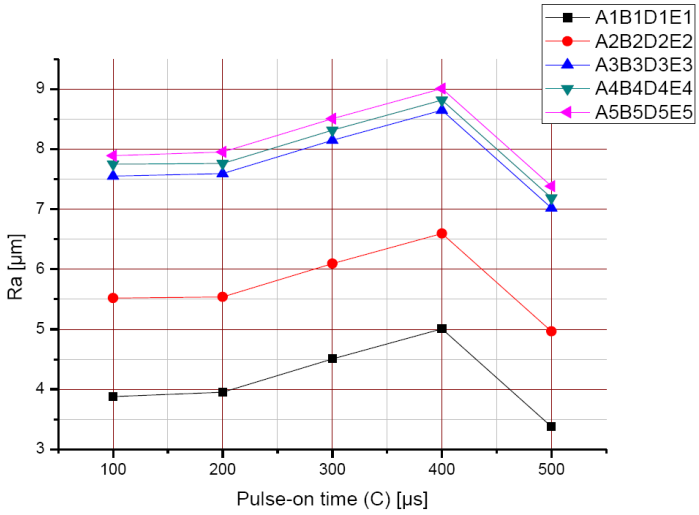

Figure 11 Effect of flushing pressure (E) on R_a (see online version for colours)

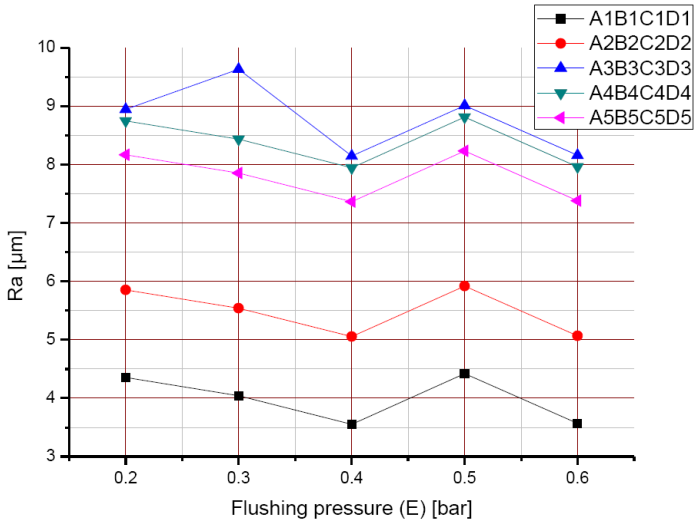

Figure 11 represents the effect of flushing pressure on R_a, while other electrical parameters viz. gap voltage, peak current, pulse-on time and duty factor have been kept constant. An approximate curve can be drawn by considering the plotted points to retrieve a trend for physically interpreting the relationship between R_a and flushing pressure. It has been inferred that with increase in flushing pressure, R_a tends to decrease. Flushing pressure helps to drain out gaseous and solid debris generated during EDM in the spark gap between workpiece and the tool electrode. As a result, increase in flushing pressure ensures efficient removal of debris by the dielectric, thereby, improving surface finish (R_a value decreases). Makenzi and Ikua (2008) reported that when the flushing pressure is too low, the flushing appears ineffective to wash out gaseous as well as eroded particles or debris completely after each discharge. However, if the pressure is excessively high, proper machining cannot be performed as the ionised plasma channel is continuously swept away. Excessive flushing pressure can also accelerate electrode wear and create turbulence in the cavity.

3.2.2 Parametric influence on SCD

EDMed end products, such as tools and dies, are often subjected to severe cyclic pressure and temperature loadings for specific applications. Hence, Thomson (1989), Zeid (1997) and Tai and Lu (2009) reported that the surface irregularities, particularly cracks, may lead to shortened service life due to reduction in material resistance to fatigue and corrosion, especially under tensile loading conditions. Therefore, surface cracks appear a fundamental consideration whilst assessing machining yield during EDM. Hence, it is indeed a necessity to understand proper controlling of process parameters to suppress their formation. The formation of surface cracks are rendered due to the differentials of high contraction stresses exceeding work material's ultimate tensile strength within the WL. Hence, it is required to understand the effect of EDM parameters of different measures of surface crack.

Figure 12 Effect of peak current (B) on SCD (see online version for colours)

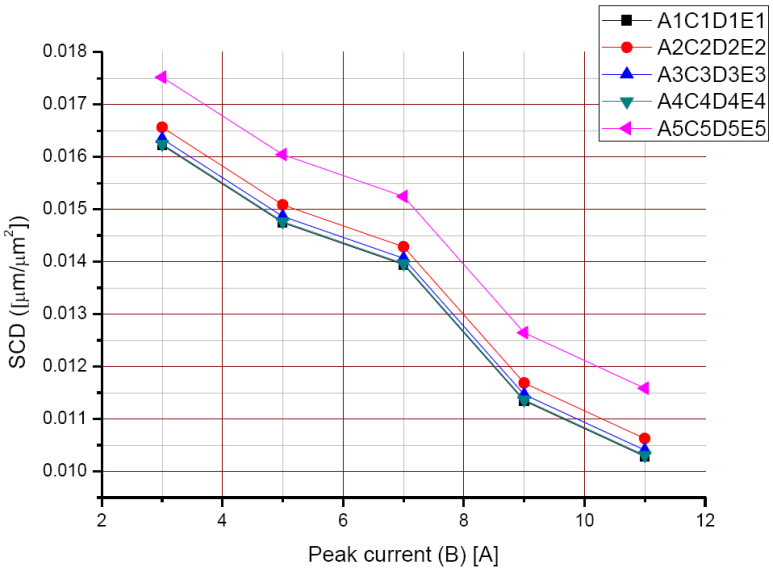

The variation of SCD with respect to change in peak current (B) has been furnished in Figure 12. For Inconel 718, trend has been observed in the manner that with increase in peak current, SCD decreases. With increase in peak current, the thickness and hence the area of WL tends to increase, resulting decrement in SCD since the length of the cracks produced does not increase in a similar rate. Lower value of SCD can also be explained due to simultaneous release of unstable energy with increase in peak current till a critical point is accomplished. However, Bhattacharyya et al. (2007) worked on EDM of M2 die steel showed that with increase in peak current, SCD decreases to some extent; then assumes gradual increment afterwards. However, within present parametric domain experimental data could retrieve only the trend of decrement of SCD with respect to increase in peak current.

Figure 13 Effect of pulse-on time (C) on SCD (see online version for colours)

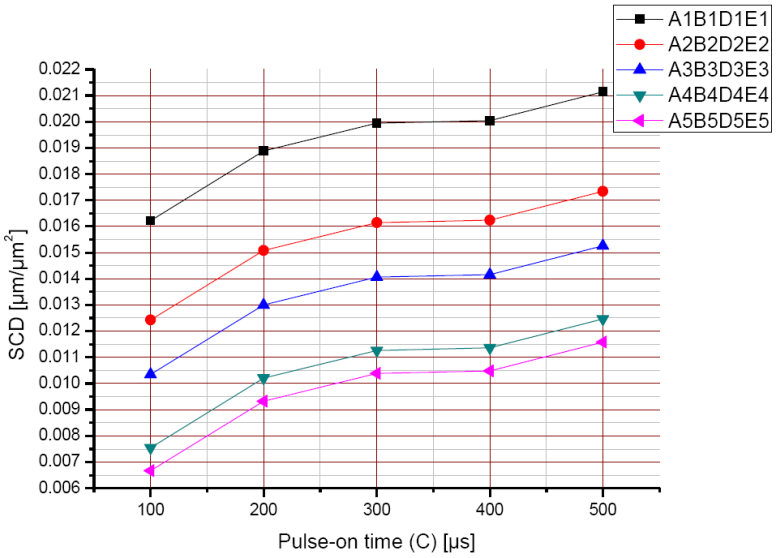

The effect of pulse-on time (C) on SCD has been demonstrated in Figure 13. With increase in pulse-on time SCD increases while other parameters kept at constant level values. Similar trend has been observed in the work by Lee and Tai (2003), Guu and Hou (2007) and Kahng and Rajukar (1977). Literature depicts that for a constant pulse current, SCD assumes an increasing trend as pulse-on time increases. Mamalis et al. (1987) and Lee et al. (1988, 1990, 1992) also reported that cracking increases as pulse energy increases. The crater size increases with increase in pulse energy; similar effect is attributed for SCD. Furthermore, the cracks penetrate into the WL and tend to propagate to depths that depend on the pulse energy.

Development of surface crack is strongly related to the EDM process parameters. Increased pulse-on duration amplify both average WLT and induced stress. As stated by Lee and Tai (2003) Rajesha et al. (2010), these two conditions stimulate crack formation. Ekmekci et al. (2005) and Mamalis et al. (1987) reported that crack density is inversely proportional to the thermal conductivity of the work material, and as the content of carbon within the WL increases from the dielectric liquid, surface crack intensity increases very rapidly. Jabbaripour et al. (2012) also reported that with increase in

pulse-on time, density of micro-holes and pits, surface cracks and irregularities, etc. increase; surface cracks in longer pulse-on time appear wider.

The effect of duty factor (D) on SCD could be well understood from Figure 14, while other parameters kept at constant level values. It has been observed that SCD gradually decreases with increase in duty factor up to certain point (duty factor 75%); then slowly assumes an increasing tend with respect to increased duty factor value. This may be explained referring to the fact that at constant gap voltage, peak-current and T_{on}, increase in duty factor results in decrease of T_{off}, which in turn reduces total cycle time (i.e., $T_{on} + T_{off}$) and thereby increases discharge frequency. The reduced T_{off} seems insufficient for subsequent cooling of molten material near the machined surface; immense heat is evolved herein which causes excess evaporation of molten material. The rate of evaporation being higher as compared to the rate of resolidification and hence, tendency to form WL; as a consequence WLT gradually reduces (Figure 17). Reduction of WL formation results in decreased SCD (Figure 14; that too, however, up to certain value of duty factor i.e., 75%. Beyond this, rate formation of WL assumes more or less constant; but intense heat generated at the machining zone (as T_{off} decreases) increases residual stress within WL. The rate of crack formation being higher; SCD gradually increases (Figure 14).

Figure 14 Effect of duty factor (D) on SCD (see online version for colours)

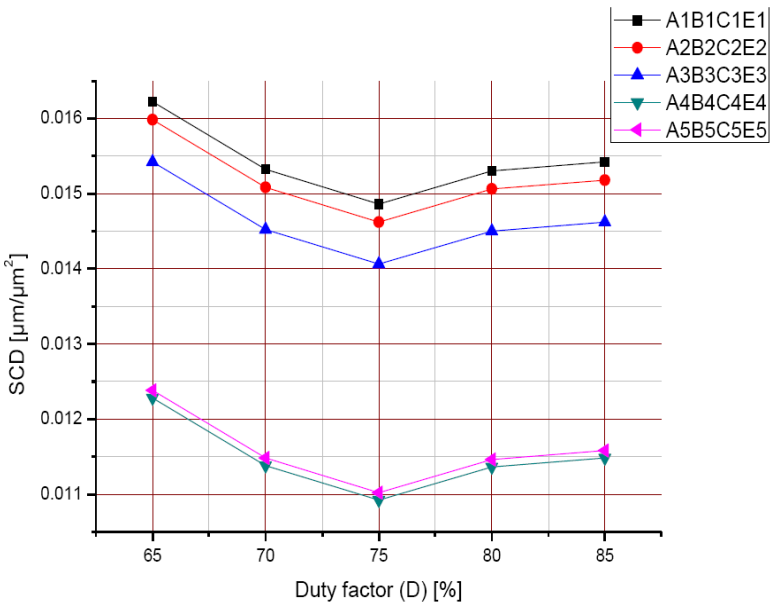

Based on Figure 15, the effect of flushing pressure on SCD on the EDMed work surface has been explained. The plots have been obtained by utilising constant parameters (electrical) parameters of EDM. An optimal dielectric flushing pressure of about 0.4bar has been noticed where the crack density assumes a minimal value. The trend of variation of SCD that could be retrieved from Figure 15 appears somewhat similar to that reported by Wong et al. (1995). While flushing pressure increases from 0.2bar to 0.4 bar, dielectric fluid appears increasingly effective in removing eroded particle from the

inter-electrode gap; this in turn reduces the possibility of WL formation and subsequent surface cracks. At low flushing pressure, the concentration of debris is high and this may stimulate preferential discharges or arcing in the territory of accumulated debris. Massive discharge rate in this region combined with enormous heat concentration due to inadequate flushing pressure of dielectric flow induce probability of surface cracking to a remarkable extent. While flushing pressure is increased beyond the optimal level, the quenching effect of dielectric onto the EDMed surface becomes more predominant. According to Lee et al. (1992), as higher heat conduction through the parent material suppress the propensity of crack formation; the higher quenching rate offered by the highly pressurised dielectric flow reduces relative heat conduction rate through the parent metal resulting more cracks at the machined surface.

Figure 15 Effect of flushing pressure (E) on SCD (see online version for colours)

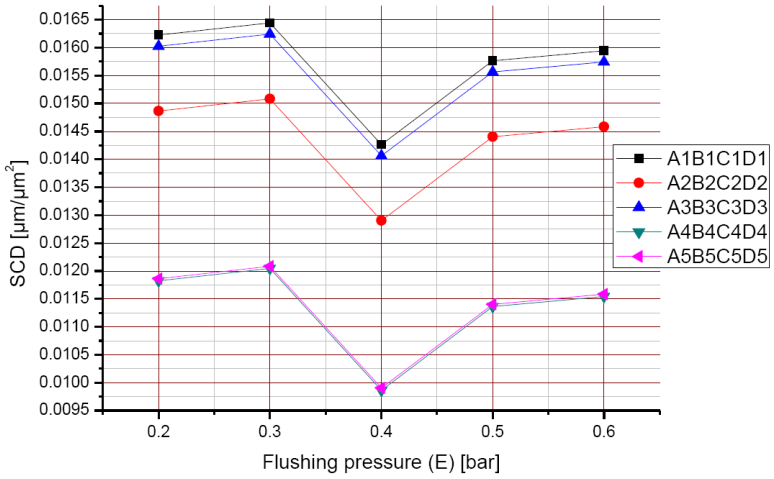

3.2.3 Parametric influence on WLT

The occurrence of spark during EDM melts and vaporises a tiny area on the surface of tool electrode. At the end of the pulse on-time, a small amount of molten material is ejected from the surface and the remaining liquid resolidifies. As explained by Tomlinson and Adkin (1992), this resolidified/recast layer is typically very fine grained and possesses high hardness as compared to the base metal, and may be alloyed with carbon from the cracked dielectric (products coming out through pyrolysis of dielectric) or with material transferred from the tool. It is also denoted as 'WL' since it remains unaffected by etching, and appears white in colour under optical microscope. As reported by Huang et al. (2004), beneath the WL, existence of a HAZ can be noticed due to the consequence of rapid heating as well as quenching cycles during EDM.

The formation of WL is incurred under different spark erosion conditions, and it exhibits surface irregularities in the form of pock marks, globules of debris, cracks and micro-cracks, whose density is greatly influenced by the process environment employed. The WL possesses high tensile residual stresses, which seems detrimental for the part functionality.

Along with various process parameters (such as gap voltage, discharge current, pulse-on time, duty factor etc.) the occurrence of WL depends on initial carbon content of the workpiece and the type of dielectric applied. Literature by Ramasawmy et al. (2005) depicts that the thickness of WL is directly dependent upon the magnitude of the pulse energy.

The WL exhibits high hardness, good adherence to the bulk and good resistance to corrosion. However, as discussed by Liao et al. (2004), WL formed by EDM process produces inferior surface finish and decreases the fatigue strength due to the presence of micro-cracks and micro-voids. Formation of WL is inevitable but highly undesirable proper controlling of EDM process parameters may reduce thickness of the WL up to certain extent. Hence, in-depth understanding of process behaviour especially, the influence of various EDM parameters on WLT appears very important. The thickness of the WL needs to be precisely controlled thus facilitating subsequent lapping process. As mentioned by Ramasawmy et al. (2005), lapping is a post-machining (post-EDM) operation to be performed to remove WL before the end product is subjected to its prescribed application domain.

Figure 16 Effect of pulse-on time (C) on WLT (see online version for colours)

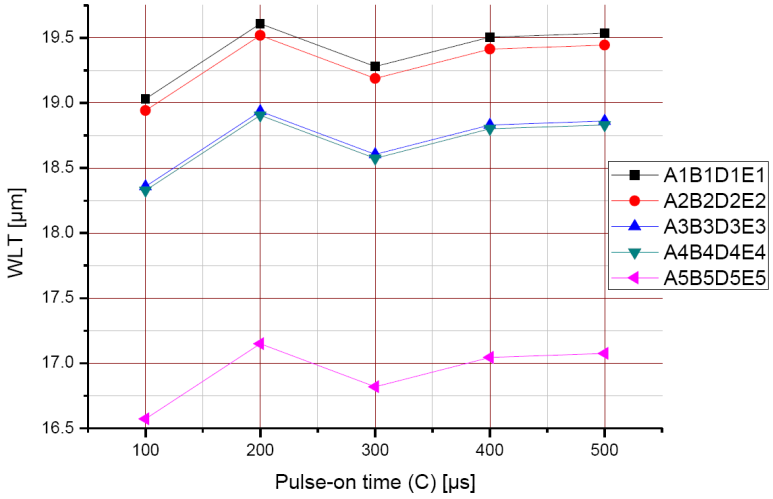

Figure 16 shows that WLT and its deviation increase with increase in pulse-on time. An average trend of upward increment has been observed for WLT with respect to the increment of pulse-on time, whilst keeping other parameters fixed at constant levels. Literature also supports that average WLT tend to increase with energy per spark, peak discharge current, and current pulse duration. According to Bozkurt et al. (1996), this could be understood by the fact that the dielectric fluid can flush out a constant amount of molten material from the machining zone, not the entire material. Therefore, as immense heat is transferred into the specimen due to increased pulse-on time, the dielectric seems unable to clear away the molten material completely; it adheres on the specimen surface. During subsequent cooling this molten material resoldifes and hence simulates formation of WL. Similar trend has also been observed in the work performed by Jabbaripour et al. (2012).

Figure 17 Effect of duty factor (D) on WLT (see online version for colours)

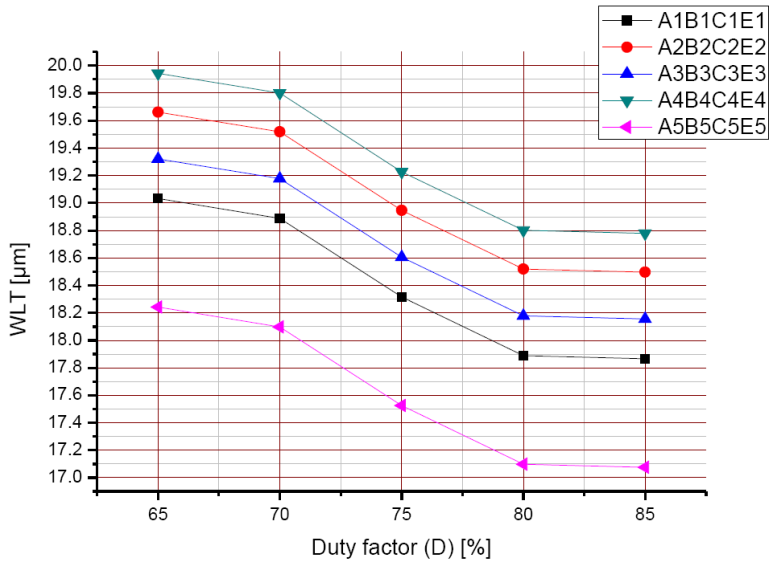

Figure 18 Effect of flushing pressure (E) on WLT (see online version for colours)

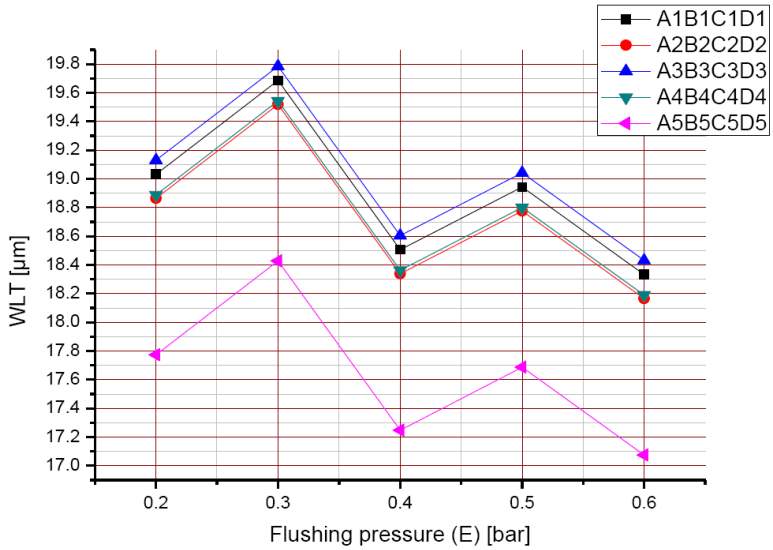

The effect of flushing pressure (E) on WLT has been shown in Figure 18. An average trend has been observed that WLT tends to decrease with increase in flushing pressure keeping other parameters set at constant level values. With increment of F_P, the effect of quenching property and debris removal capability of the dielectric fluid becomes predominant, thereby; chance of WL growth diminishes.

3.3 Optimisation of machining responses

3.3.1 Methodology: utility theory combined with Taguchi method

As described by Walia et al. (2006) and Singh and Kumar (2006), utility can be defined as the usefulness of a product/process with reference to the customers' expectations. A product/process is characterised by several performance measures of conflicting requirements [ex. higher-is-better (HB); lower-is-better (LB)]. The advantage of utility theory is to aggregate utility of individual performances features into a unique index called overall utility degree. The best product/process should correspond to the maximum overall utility.

Therefore, the overall usefulness of a product can be assessed by overall utility degree which is the sum of the individual utilities of various performance characteristics of the product/process.

Assuming an EDM process is characterised by a total K performance attributes (ex. $K = 3$; i.e., R_a, SCD and WLT, in the present case); and, a total N settings (parametric combinations) are available for evaluation (ex. $N = 25$; in the present case). The 25 parametric combinations of L_{25} OA are nothing but possible process environments; can be understood as candidate alternatives. Each process environment is capable of providing performance outputs. The goal of adopting utility theory is to select the best process environment to satisfy contradicting requirements of multi-performance yields simultaneously for the EDM process.

If $x_i(k)$ is the measure of effectiveness (experimental data) of k^{th} attribute (or performance characteristic) in i^{th} experimental run ($I = 1,2\ldots,N$) and there exists a total of K attributes evaluating the outcome space, then the joint utility function can be expressed as:

$$U_o\left(x(1), x(2),\ldots, x(k),\ldots, x(K)\right) = f\left(U(1), U(2),\ldots, U(k),\ldots U(K)\right) \tag{1}$$

A preference scale for each performance attribute is constructed for determining its utility value. Two arbitrary numerical values (preference number) 0 and 9 are assigned to the just acceptable (the worst) and the most acceptable (the best) value of the performance attribute, respectively. The preference number (also called utility value) of a particular response can be expressed on a logarithmic scale as follows.

$$U_i(k) = A \times \log\left(\frac{x_i(k)}{\overline{x}(k)}\right) \tag{2}$$

Here $U_i(k)$ denotes utility value of k^{th} attribute in i^{th} setting; is the value of k^{th} performance attribute obtained at i^{th} setting; where, ($k = 1,2,\ldots K$) and ($i = 1,2,\ldots,N$).

Also, $\overline{x}(k)$ is the just acceptable value of k^{th} performance attribute with the following condition i.e.,

- $\overline{x}(k) = \underset{i=1,2,\ldots,N}{Min}[x_i(k)]$, if the requirement of k^{th} performance attribute is HB; else,

- $\bar{x}(k) = \underset{i=1,2,\ldots,N}{Max}[x_i(k)]$, if the requirement of k^{th} performance attribute is LB.

The value of A can be found by utilising two boundary conditions that:

$$\text{if } x_i(k) = \bar{x}(k) \Rightarrow U_i(k) = (0)$$

$$\text{and if } x_i(k) = x^*(k) \Rightarrow U_i(k) = 9.$$

Here,

- $x^*(k) = \underset{i=1,2,\ldots,N}{Max}[x_i(k)]$, if the requirement of k^{th} performance attribute is HB; else
- $x^*(k) = \underset{i=1,2,\ldots,N}{Min}[x_i(k)]$, if the requirement of k^{th} performance attribute is LB; $x^*(k)$ being the most acceptable value for k^{th} performance attribute.

Therefore,

$$A = \frac{9}{\log\left(\frac{x^*(k)}{\bar{x}(k)}\right)} \tag{3}$$

The overall utility degree U_i^O for i^{th} process environment can be calculated as follows. (assuming equal priority weight of individual attributes).

$$U_i^O = \frac{1}{K}\sum_{k=1}^{K} U_i(k); (i = 1,2,\ldots,N; k = 1,2,\ldots,K) \tag{4}$$

Based on U_i^O, the superiority of performance can be well articulated for the setting which corresponds to maximum U_i^O, and, this setting can be treated as optimal setting. However, in the present work, the most favourable setting (with maximum U_i^O) can easily be identified from amongst 25 settings experimented as per L_{25} OA. But this setting cannot be treated as optimal because there may be a possibility that the maximum U_i^O may be obtained at a different setting beyond L_{25} OA since full factorial designed experimentation is not performed. Therefore, overall utility thus obtained from L_{25} OA experimentation needs to be extrapolated. This can be done by Taguchi method. Hence, the advantage of exploring utility theory can be well understood by the fact that utility theory provides a basis for logical aggregation of multi-performance features into a single performance index thus providing scope for applying Taguchi method for optimisation; because, traditional Taguchi method fails to solve multi-response optimisation problem. Utility theory eliminates dimensional effect and criteria conflict and combines utility values of individual responses into overall utility which corresponds to HB requirement.

Table 5 Utility values of individual responses: computed values of overall utility degree and corresponding S/N ratio

Sl. no.	*Individual utility degree*			*Overall utility degree, U_o*	*Corresponding S/N ratio [dB]*	*Predicted S/N ratio at optimal setting [dB]*
	URa	*USCD*	*UWLT*			
1	5.706	1.326	2.396	3.1393	9.9367	19.7934
2	2.793	0.960	1.659	1.8022	5.1161	
3	0.704	1.661	8.170	3.5082	10.9017	
4	0.263	2.435	3.986	2.2259	6.9501	
5	1.752	2.168	6.306	3.4052	10.6429	
6	5.808	1.515	2.837	3.3833	10.5868	
7	4.870	1.612	7.875	4.7808	13.5900	
8	1.412	1.612	6.676	3.2302	10.1846	
9	1.702	1.420	0.000	1.0396	0.3373	
10	0.420	9.000	6.114	5.1728	14.2745	
11	7.118	0.000	1.007	2.7056	8.6453	
12	3.563	1.095	0.488	1.7137	4.6787	
13	2.008	0.871	0.466	1.1140	0.9377	
14	1.092	5.247	1.965	2.7653	8.8348	
15	0.341	3.059	2.809	2.0676	6.3093	
16	5.045	0.697	4.688	3.4731	10.8143	
17	3.844	1.373	5.292	3.4994	10.8799	
18	2.061	4.141	5.117	3.7691	11.5248	
19	3.426	6.000	3.799	4.4041	12.8771	
20	0.263	4.005	3.408	2.5562	8.1519	
21	9.000	1.420	6.472	5.6251	15.0026	
22	3.426	3.548	9.000	5.3196	14.5176	
23	1.956	2.435	6.203	3.5280	10.9506	
24	0.662	3.612	1.256	1.8418	5.3048	
25	0.000	4.710	2.830	2.5109	7.9966	

Table 6 Mean response (S/N ratio of overall utility degree) table: prediction of optimal setting by optimising U_o

Levels of variation	*Mean S/N ratio values at different factorial levels*				
	A	*B*	*C*	*D*	*E*
1	8.709	10.997	11.818	6.811	8.523
2	9.795	9.756	9.168	7.289	6.724
3	5.881	8.900	9.319	9.840	11.547
4	10.850	6.861	8.125	10.675	8.229
5	10.754	9.475	7.560	11.373	10.967
Delta (Max-Min)	4.968	4.136	4.258	4.562	4.823
Rank	1	5	4	3	2

3.3.2 Results: evaluation of optimal setting

Experimentally obtained response data have been utilised to compute utility values of individual responses (R_a, SCD and WLT). In this computation, utility degrees of individual responses have been computed based on LB criterion [equation (2)] and shown in Table 5. Assuming equal priority weight of the responses, overall utility index (U_O) has been computed [using equation (4)] for all experimental runs; values have been provided in Table 5. The overall utility has been treated as single objective function and finally optimised (maximised) by Taguchi method. Table 6 exhibits mean response (S/N ratio of overall utility) values for different factorial settings; the same has been plotted in Figure 19. The optimal setting appears as $A_4B_1C_1D_5E_3$ i.e., (V_g = 80 V; I_P = 3 A; T_{on} = 100 μs; τ = 85%; F_P = 0.4 bar). The predicted S/N ratio value of U_O at optimal setting corresponds to a value of 19.7934 dB which seems more as compared to the S/N ratios of U_O obtained in all 25 experimental runs (Table 5). As S/N ratio dictates its requirement of HB type; the highest S/N ratio of U_O at optimal setting confirms Taguchi's prediction to a reliable extent. This has further been verified by confirmatory test.

Figure 19 Mean S/N ratio (of overall utility degree) plot: predicted optimal setting = $A_4B_1C_1D_5E_3$ i.e., [V_g = 80V; I_P = 3A; T_{on} = 100 μs; τ = 85%; F_P = 0.4bar] (see online version for colours)

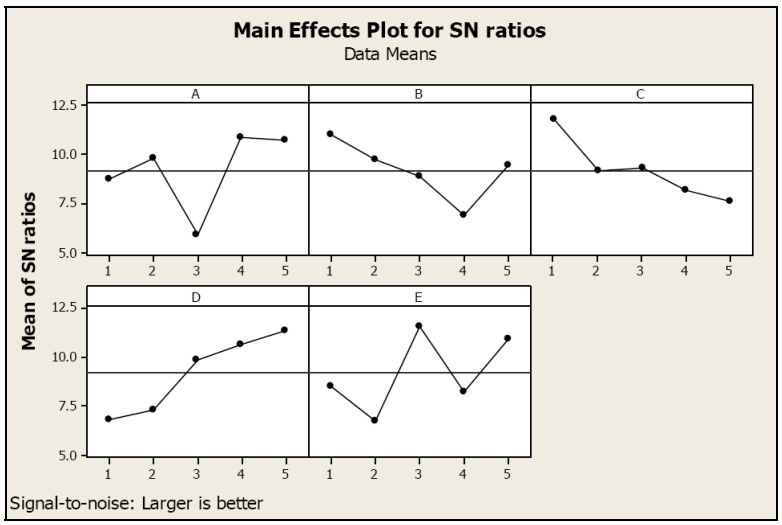

4 Conclusions

Within scope and limitation of the present research, the following conclusions have been drawn.

1 Alteration of chemical composition due to pyrolysis of dielectric fluid has been observed for EDMed Inconel 718 specimens. Increased carbon content at the machined surface results an increase in micro-hardness value as compared to the base metal. However, micro-hardness of the WL has been found to vary (within

352.600 $HV_{0.05}$ to 269.400 $HV_{0.05}$) depending on the parameters setting utilised during EDM.

2 Surface morphology of EDMed Inconel 718 has been characterised by the presence of surface cracks, cracker, globule of debris, pockmarks etc. whose intensity tend to vary depending on parameters settings. Two different types of cracks have been identified in the machined specimen.

3 Direct effect of process parameters on R_a, SCD and thickness of WL have been demonstrated herein along with physical explanations.

4 It has been observed that thermo-mechanical phenomena during EDM process induce residual stress within the specimen. The residual stress induced within the EDMed specimen appears higher as compared to that of parent material (as received). Evolution of residual stress during machining promotes crack formation and subsequent propagation.

5 XRD analysis of EDMed Inconel 718 exhibited surface structure of cubic FCC matrix consisting of Ni-based solid solution with precipitates of $Cr_{23}C_6$ (chromium carbide), MoC (molybdenum carbide) and Nb_2C (niobium carbide). Grain refinement has also been observed during EDM of Inconel 718.

6 In relation of the setup utilised in this research and within selected experimental domain, the most favourable (optimal) process environment appears as: [V_g = 80V; I_P = 3A; T_{on} = 100μs; τ = 85%; F_P = 0.4bar] which is expected to satisfy requirements of multi-responses, simultaneously. Confirmatory test depicted that predicted optimal parameters setting is capable of minimising R_a, SCD and WLT, simultaneously, up to maximum possible extent. Aforesaid work highlights application of utility theory integrated with Taguchi method for solving such a multi-response optimisation problem.

Acknowledgements

We hereby express our heartfelt thanks to Prof. M.A. Dorgham, the Editor-in-Chief of *International Journal of Materials and Product Technology* (IJMPT) and also the anonymous learned reviewers for their valuable comments and suggestions to make our paper a good contributor.

References

Aggarwal, V., Khangura, S.S. and Garg, R.K. (2015) 'Parametric modeling and optimization for wire electrical discharge machining of Inconel 718 using response surface methodology', *International Journal of Advanced Manufacturing Technology*, Vol. 79, No. 1, pp.31–47.

Ay, M., Çaydaş, U. and Hasçalık, A. (2013) 'Optimization of micro-EDM drilling of Inconel 718 super alloy', *International Journal of Advanced Manufacturing Technology*, Vol. 66, No. 5, pp.1015–1023.

Bhattacharyya, B., Gangopadhyay, S. and Sarkar, B.R. (2007) 'Modelling and analysis of EDM ED job surface integrity', *Journal of Materials Processing Technology*, Vol. 189, No. 1, pp.169–177.

Bozkurt, B., Gadalla, A.M. and Eubank, P.T. (1996) 'Simulation of erosions in a single discharge EDM process', *Material and Manufacturing Process*, Vol. 11, No. 4, pp.555–563.

Crookall, J.R. and Khor, B.C. (1975) 'Electro-discharge machined surfaces', *Proceedings of the Fifteenth International Machine Tool Design and Research Conference*, Macmillan Education, UK, pp.373–384.

Dhanabalan, S., Sivakumar, K. and Narayanan, C.S. (2014) 'Analysis of form tolerances in electrical discharge machining process for Inconel 718 and 625', *Materials and Manufacturing Processes*, Vol. 29, No. 3, pp.253–259.

Ekmekci, B. (2007) 'Residual stresses and white layer in electric discharge machining (EDM)', *Applied Surface Science*, Vol. 253, No. 23, pp.9234–9240.

Ekmekci, B. (2009) 'White layer composition, heat treatment, and crack formation in electric discharge machining process', *Metallurgical and Materials Transactions B*, Vol. 40, No. 1, pp.70–81.

Ekmekci, B., Elkoca, O., Erman Tekkaya, A. and Erden, A. (2005) 'Residual stress state and hardness depth in electric discharge machining: de-ionized water as dielectric liquid', *Machine Science and Technology*, Vol. 9, No. 1, pp.39–61.

Ekmekci, B., Tekkaya, A.E. and Erden, A. (2006) 'A semi-empirical approach for residual stresses in electric discharge machining (EDM)', *International Journal of Machine Tools and Manufacture*, Vol. 46, No. 7, pp.858–868.

Guu, Y.H. and Hocheng, H. (2001) 'Effects of workpiece rotation on machinability during electrical-discharge machining', *Materials and Manufacturing Processes*, Vol. 16, No. 1, pp.91–101.

Guu, Y.H. and Hou, M.T.K. (2007) 'Effect of machining parameters on surface textures in EDM of Fe-Mn-Al alloy', *Materials Science and Engineering: A*, Vol. 466, No. 1, pp.61–67.

Guu, Y.H., Chou, C.Y. and Chiou, S.T. (2005) 'Study of the effect of machining parameters on the machining characteristics in electrical discharge machining of Fe-Mn-Al alloy', *Materials and Manufacturing Processes*, Vol. 20, No. 6, pp.905–916.

Hasçalýk, A. and Çaydaş, U. (2004) 'Experimental study of wire electrical discharge machining of AISI D5 tool steel', *Journal of Materials Processing Technology*, Vol. 148, No. 3, pp.362–367.

Hewidy, M.S., El-Taweel, T.A. and El-Safty, M.F. (2005) 'Modelling the machining parameters of wire electrical discharge machining of Inconel 601 using RSM', *Journal of Materials Processing Technology*, Vol. 169, No. 2, pp.328–336.

Huang, C.A., Hsu, F.Y. and Yao, S.J. (2004) 'Microstructure analysis of the martensitic stainless steel surface fine-cut by the wire electrode discharge machining (WEDM)', *Materials Science and Engineering: A*, Vol. 371, No. 1, pp.119–126.

Huang, J.T., Liao, Y.S. and Hsue, W.J. (1999) 'Determination of finish-cutting operation number and machining-parameters setting in wire electrical discharge machining', *Journal of Materials Processing Technology*, Vol. 87, No. 1, pp.69–81.

Jabbaripour, B., Sadeghi, M.H., Faridvand, S. and Shabgard, M.R. (2012) 'Investigating the effects of EDM parameters on surface integrity, MRR and TWR in machining of Ti-6Al-4V', *Machining Science and Technology*, Vol. 16, No. 3, pp.419–444.

Kahng, C.H. and Rajurkar, K.P. (1977) 'Surface characteristics behaviour due to rough and fine cutting by EDM', *Annals of the CIRP*, Vol. 26, No. 1, pp.77–82.

Keskin, Y., Halkacı, H.S. and Kizil, M. (2006) 'An experimental study for determination of the effects of machining parameters on surface roughness in electrical discharge machining (EDM)', *International Journal of Advanced Manufacturing Technology*, Vol. 28, Nos. 11–12, pp.1118–1121.

Kruth, J.P. and Bleys, P. (2000) 'Measuring residual stress caused by wire EDM of tool steel', *International Journal of Electrical Machining*, Vol. 5, pp.23–28.

Kumar, A., Maheshwari, S., Sharma, C. and Beri, N. (2011) 'Analysis of machining characteristics in additive mixed electric discharge machining of Nickel-based super alloy Inconel 718', *Materials and Manufacturing Processes*, Vol. 26, No. 8, pp.1011–1018.

Lee, H.T. and Tai, T.Y. (2003) 'Relationship between EDM parameters and surface crack formation', *Journal of Materials Processing Technology*, Vol. 142, No. 3, pp.676–683.

Lee, H.T. and Yur, J.P. (2000) 'Characteristic analysis of EDMed surfaces using the Taguchi approach', *Materials and Manufacturing Processes*, Vol. 15, No. 6, pp.781–806.

Lee, L.C., Lim, L.C. and Wong, Y.S. (1992) 'Towards crack minimisation of EDMed surfaces', *Journal of Materials Processing Technology*, Vol. 32, Nos. 1–2, pp.45–54.

Lee, L.C., Lim, L.C., Narayanan, V. and Venkatesh, V.C. (1988) 'Quantification of surface damage of tool steels after EDM', *International Journal of Machine Tools and Manufacture*, Vol. 28, No. 4, pp.359–372.

Lee, L.C., Lim, L.C., Wong, Y.S. and Lu, H.H. (1990) 'Towards a better understanding of the surface features of electro-discharge machined tool steels', *Journal of Materials Processing Technology*, Vol. 24, pp.513–523.

Li, L., Li, Z.Y., Wei, X.T. and Cheng, X. (2015) 'Machining characteristics of Inconel 718 by sinking-EDM and wire-EDM', *Materials and Manufacturing Processes*, Vol. 30, No. 8, pp.968–973.

Liao, Y.S., Huang, J.T. and Chen, Y.H. (2004) 'A study to achieve a fine surface finish in wire-EDM', *Journal of Materials Processing Technology*, Vol. 149, No. 1, pp.165–171.

Lin, M-Y., Tsao, C-C., Hsu, C-Y., Chiou, A-H., Huang, P-C. and Lin, Y-C. (2013) 'Optimization of micro milling electrical discharge machining of Inconel 718 by Grey-Taguchi method', *Transactions of Nonferrous Materials Society China*, Vol. 23, No. 3, pp.661–666.

Makenzi, M.M. and Ikua, B.W. (2012) 'A review of flushing techniques used in electrical discharge machining', *Proceedings of the 2012 Mechanical Engineering Conference on Sustainable Research and Innovation*, 3–4 May, Vol. 4.

Mamalis, A.G., Vosniakos, G.C., Vaxevanidis, N.M. and Prohaszka, J. (1987) 'Macroscopic and microscopic phenomena of electro-discharge machined steel surfaces: an experimental investigation', *Journal of Mechanical Working Technology*, Vol. 15, No. 3, pp.335–356.

Newton, T.R., Melkote, S.N., Watkins, T.R., Trejo, R.M. and Reister, L. (2009) 'Investigation of the effect of process parameters on the formation and characteristics of recast layer in wire-EDM of Inconel 718', *Materials Science and Engineering A*, Vols. 513–514, pp.208–215.

Ogata, I. and Mukoyama, Y. (1991) 'Residual stress on surface machined by wire electric discharge', *International Journal of the Japan Society for Precision Engineering*, Vol. 25, No. 4, pp.273–278.

Opitz, H. (1960) 'Metallurgical aspects and surface characteristics', *Proceedings of Spark Machining Symposium*, Birmingham, UK, pp.237–251.

Prihandana, G.S., Sriani, T., Mahardika, M., Hamdi, M., Miki, N., Wong, Y.S. and Mitsui, K. (2014) 'Application of powder suspended in dielectric fluid for fine finish micro-EDM of Inconel 718', *International Journal of Advanced Manufacturing Technology*, Vol. 75, No. 1, pp.599–613.

Rajesha, S., Sharma, A.K. and Kumar, P. (2010) 'Some aspects of surface integrity study of electro discharge machined Inconel 718', *Proceedings of the 36th International MATADOR Conference*, Springer, London, pp.439–444.

Rajesha, S., Sharma, A.K. and Kumar, P. (2012) 'On electro discharge machining of Inconel 718 with hollow tool', *Journal of Materials Engineering and Performance*, Vol. 21, No. 6, pp.882–891.

Ramakrishnan, R. and Karunamoorthy, L. (2008) 'Modeling and multi-response optimization of Inconel 718 on machining of CNC WEDM process', *Journal of Materials Processing Technology*, Vol. 207, Nos. 1–3, pp.343–349.

Ramasawmy, H., Blunt, L. and Rajurkar, K.P. (2005) 'Investigation of the relationship between the white layer thickness and 3D surface texture parameters in the die sinking EDM process', *Precision Engineering*, Vol. 29, No. 4, pp.479–490.

Rao, G.K.M., Satyanarayana, S. and Praveen, M. (2008) 'Influence of machining parameters on electric discharge machining of maraging steels – an experimental investigation', *Proceedings of the World Congress on Engineering*, Vol. 2, WCE 2008, London, UK, 2–4 July.

Rebelo, J.C., Dias, A.M., Kremer, D. and Lebrun, J.L. (1998) 'Influence of EDM pulse energy on the surface integrity of martensitic steels', *Journal of Materials Processing Technology*, Vol. 84, No. 1, pp.90–96.

Saha, S.K. and Choudhury, S.K. (2009) 'Experimental investigation and empirical modelling of the dry electric discharge machining process', *International Journal of Machine Tools and Manufacture*, Vol. 49, Nos. 3–4, pp.297–308.

Simao, J., Lee, H.G., Aspinwall, D.K., Dewes, R.C. and Aspinwall, E.M. (2003) 'Workpiece surface modification using electrical discharge machining', *International Journal of Machine Tools and Manufacture*, Vol. 43, No. 2, pp.121–128.

Singh, H. and Kumar, P. (2006) 'Optimizing multi-machining characteristics through Taguchi's approach and utility concept', *Journal of Manufacturing Technology Management*, Vol. 17, No. 2, pp.255–274.

Tai, T.Y. and Lu, S.J. (2009) 'Improving the fatigue life of electro-discharge-machined SDK11 tool steel via the suppression of surface cracks', *International Journal of Fatigue*, Vol. 31, No. 3, pp.433–438.

Thomson, P.F. (1989) 'Surface damage in electro-discharge machining', *Materials Science and Technology*, Vol. 5, No. 11, pp.1153–1157.

Tomlinson, W.J. and Adkin, J.R. (1992) 'Microstructure and properties of electro discharge machined surfaces', *Surface Engineering*, Vol. 8, No. 4, pp.283–288.

Tönshoff, H.K. and Brinksmeier, E. (1980) 'Determination of the mechanical and thermal influences on machined surfaces by microhardness and residual stress analysis', *CIRP Annals-Manufacturing Technology*, Vol. 29, No. 2, pp.519–530.

Tsai, H.C., Yan, B.H. and Huang, F.Y. (2003) 'EDM performance of Cr/Cu-based composite electrodes', *International Journal of Machine Tools and Manufacture*, Vol. 43, No. 3, pp.245–252.

Walia, R.S., Shan, H.S. and Kumar, P. (2006) 'Multi-response optimization of CFAAFM process through Taguchi method and utility concept', *Materials and Manufacturing Processes*, Vol. 21, No. 8, pp.907–914.

Williams, R.E. and Rajurkar, K.P. (1991) 'Study of wire electrical discharge machined surface characteristics', *Journal of Materials Processing Technology*, Vol. 28, Nos. 1–2, pp.127–138.

Wong, Y.S., Lim, L.C. and Lee, L.C. (1995) 'Effects of flushing on electro-discharge machined surfaces', *Journal of Materials Processing Technology*, Vol. 48, No. 1, pp.299–305.

Yan, B.H., Tsai, H.C. and Huang, F.Y. (2005) 'The effect in EDM of a dielectric of a urea solution in water on modifying the surface of Titanium', *International Journal of Machine Tools and Manufacture*, Vol. 45, No. 2, pp.194–200.

Yildiz, Y., Sundaram, M.M., Rajurkar, K.P. and Altintas, A. (2015) 'Correlation of surface roughness and recast layer thickness in electrical discharge machining', *Proceedings of the Institution of Mechanical Engineers, Part E: Journal of Process Mechanical Engineering*, [online] doi/abs/10.1177/0954408915600949, http://journals.sagepub.com.

Zeid, O.A. (1967) 'On the effect of electro-discharge machining parameters on the fatigue life of AISI D6 tool steel', *Journal of Materials Processing Technology*, Vol. 68, No. 1, pp.27–32.